Automated Detection of Field Match Lines between Supraclavicular and Tangent Irradiation Fields with Cherenkov Imaging

JULY 12–16 2020 VIRTUAL
JOINT AAPM | COMP MEETING
EASTERN TIME [GMT-4]

R. HACHADORIAN [1], P. BRUZA[2], M. JERMYN, D. GLADSTONE, B.POGUE, L. JARVIS
1 Thayer School of Engineering, Dartmouth College, Hanover, NH USA
2 DoseOptics LLC, Lebanon, NH USA
3 Geisel School of Medicine, Hanover, NH USA
4 Norris Cotton Cancer Center, Dartmouth-Hitchcock Medical Center, Lebanon, NH USA

INTRODUCTION

In monoisocentric radiation therapy treatment plans designed to treat the whole breast and the supraclavicular lymph nodes, the nodal fields abut the whole breast fields at the isocenter, forming the match line. Insufficient coverage at the field match line can lead to recurrence, and field overlap over weeks of treatment can lead to increased risk of healthy tissue damage. The value of Cherenkov imaging at the field junction was completed to assess the accuracy of identifying potential incidents with this new imaging technology.

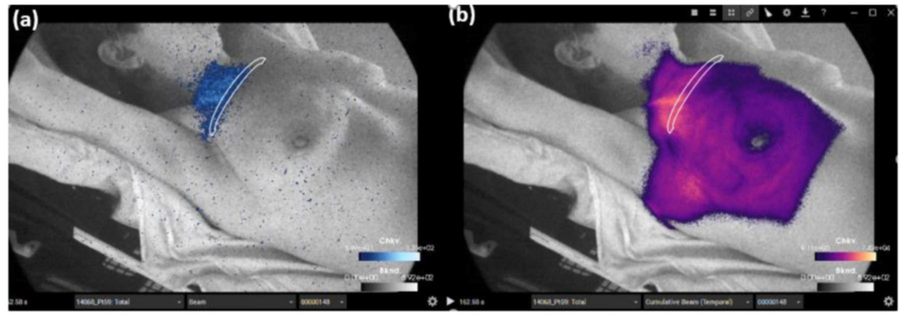

FIGURE 1: In this fraction of recorded treatment, the supraclavicular field is delivered, followed by the tangent fields (a). The cumulative image (b) shows the treatment as the frames are summed temporally.

AIM

In patient verification, complexities include analyzing fields from diverging beams that are summed from non-rectangular fields, over geometries that are not flat, so there is an existing deficit in literature for field match analysis in the complexity of human radiation treatments. The methods developed in this study result in a match line finding technique sensitive to subtle changes due to slight misalignments, breathing or changes in anatomy. This study is the first to develop an automated methodology for isolating straight-abutting regions of field match, and systematically examine it in anthropomorphic phantoms and human patients during radiotherapy treatments.

METHODS

First, a controlled study was conducted by modifying a patient treatment plan to iteratively increase overlap or gap between tangent and supraclavicular fields, then delivering the plan to an anthropomorphic phantom. By applying an intensity threshold to the product of the two deconvolved Cherenkov images, the region of field match could be isolated using automated techniques and the meeting point of their profiles assessed. These methods were then applied to three patients.

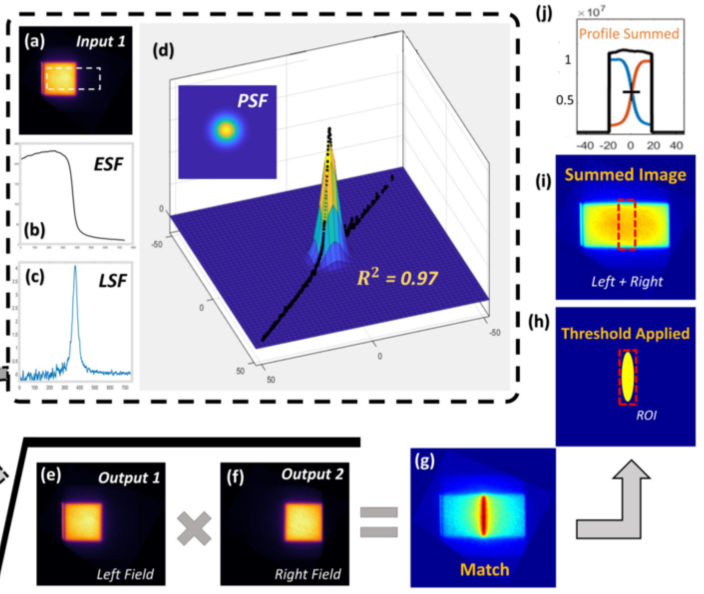

FIGURE 2: In (a), an ROI is taken from an input image and vertically summed to create the edge spread function (ESF) in (b) which is differentiated to view the line spread function (LSF) in (c). A 2D gaussian was fit using the LSF as a cross-section (d) to yield the point spread function, (PSF). The PSF is then used to deconvolve the left field (a) and right field (not shown), to get left field outputs (e) and right field outputs (f). The product and square root of both output images forms the match or product image (g). An intensity threshold was applied to create the yellow mask in (h) where automated techniques isolated the rectangular ROI (red) circumscribing the threshold mask. This region becomes the mask for the output images in (i), resulting in their respective profiles (j). Match amplitude is indicated by central crosshair.

RESULTS

The intersection point between matching field profiles was directly correlated to the distance (gap/overlap) between the fields (anthropomorphic phantom R^2 = 0.994 "breath hold" and R^2 = 0.990 "free breathing"). The profile intersection points from three patients' imaging sessions were then evaluated similarly for inter-fraction consistency.

Treatment analysis completed on patients found that the match point offsets fell within 2.5 mm when using the anthropomorphic phantom as a means of calibration; a physically reasonable range.

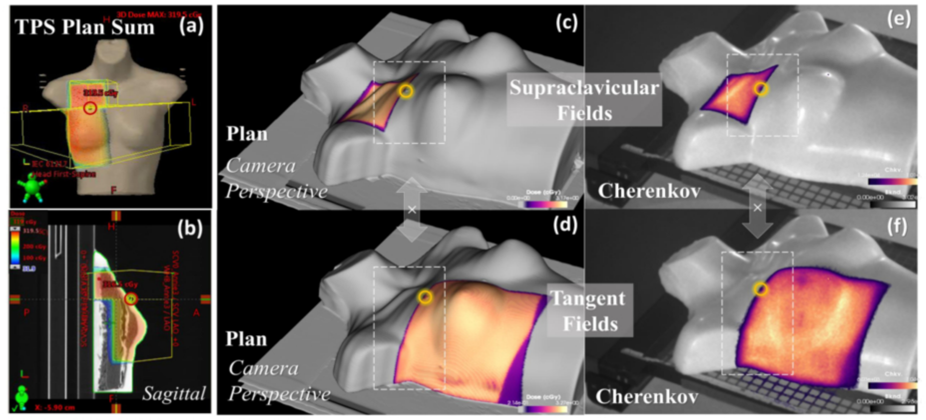

FIGURE 4: Subfigure (a) provides a coronal-view screenshot of the delivered treatment plan, consisting of two supraclavicular beams (AP/PA), shown superior to the tangent fields (RPO/LAO), meeting at isocenter (red). In (b), the sagittal view (TPS) is shown. The plan information was exported from the TPS and rendered in the view of the Cherenkov camera in (c) for supraclavicular fields and (d) for tangent fields. Their respective, cumulative Cherenkov images are shown in (e) and (f), isocenter circled in yellow.

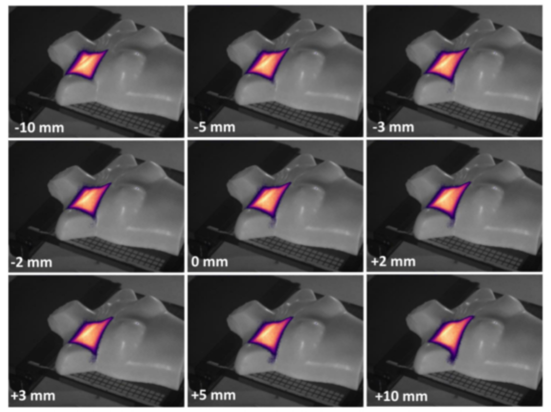

FIGURE 5: The supraclavicular fields for introduced gap are seen with 10 mm of separation, 5 mm, 3 mm and 2 mm (denoted minus sign). The 0 mm match SCV field is centered, then is followed by introduced overlaps of 2 mm, 3 mm, 5 mm, 10 mm., and introduced overlap (denoted plus sign). These measurements are used to generate the calibration in Figure 6.

FIGURE 6: The Cherenkov match images and field sums were transformed to an en face view for fields with added (a) separation, (b) true match, and (c) overlap. These images have been rotated 90 degrees, column summed, and normalized such that the tangent field (blue) summed with the supraclavicular field (orange) yields the profile sum (black), with match/intersection point denoted by crosshair. In (d) a fit was applied between overlap distance and match point height for breath hold treatment (blue), and free breathing treatment (orange).

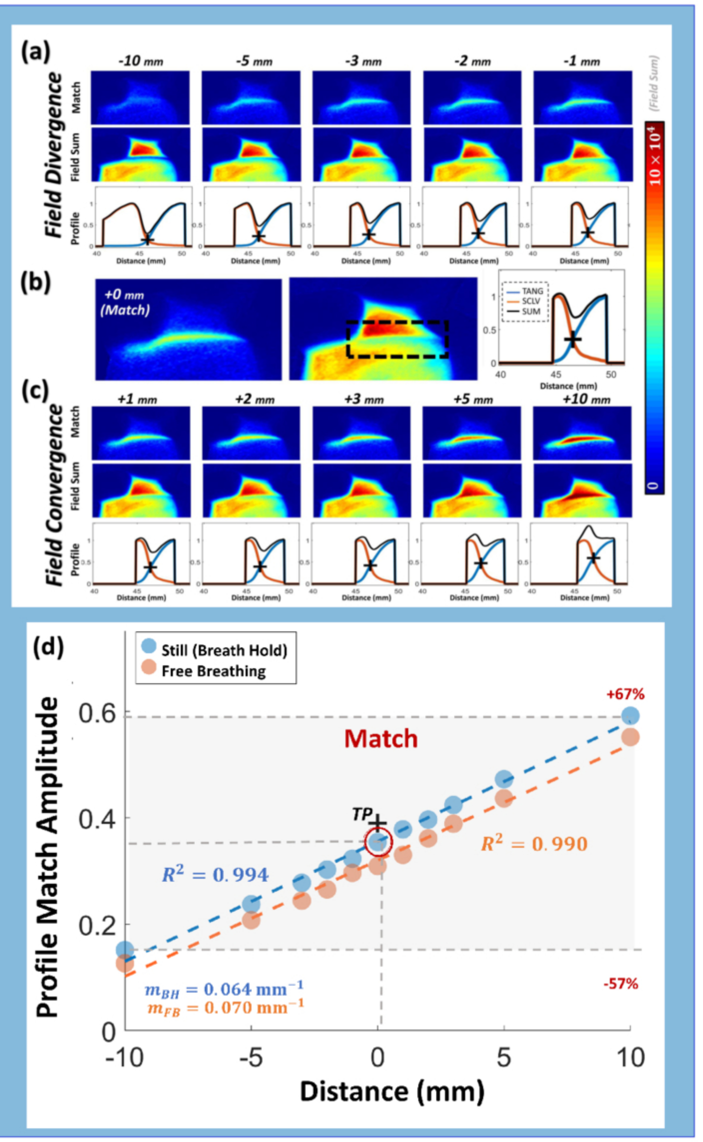

FIGURE 7: In (a), both RPO and LAO supraclavicular (SCV) fields from the treatment plan are shown. In (b), the same is shown for all four tangent fields RPO/LAO 6X/10X summed. The match (product) image is shown in (c), followed by the treatment plan profile (d). In (e) the supraclavicular Cherenkov image and (f) the tangent fields Cherenkov image are shown from day one of the patient's treatment. Likewise, the Cherenkov match image (g) and the respective profile are shown (h). In (i), the Cherenkov images and profiles are shown for the next four fractions of treatment. In (j) the ratio of the Cherenkov image match amplitude over the TPS match amplitude is plotted with respect to recorded treatment day. The range of gaps and overlaps spanned 1.8 mm surrounding the expectation from the treatment plan.

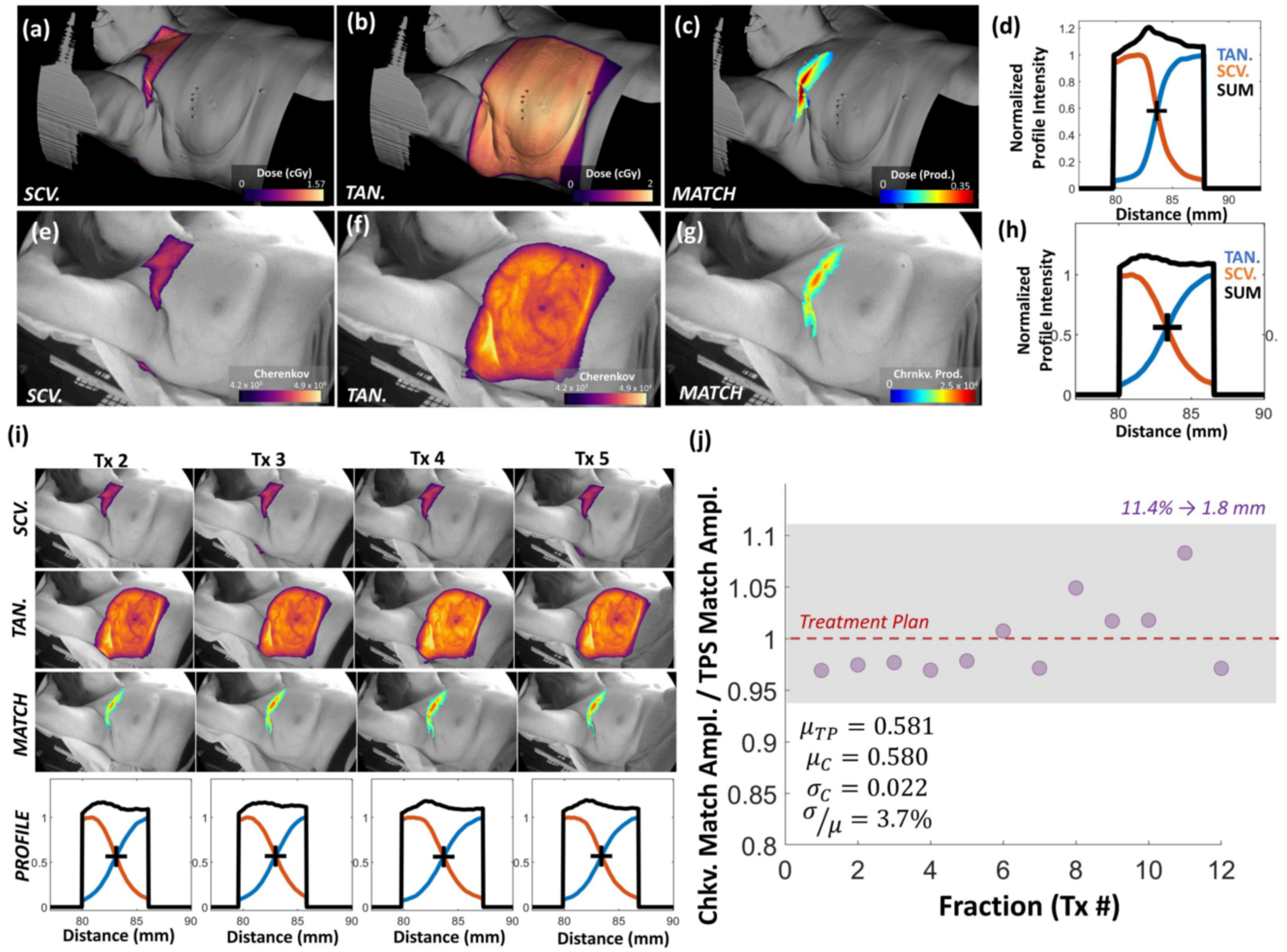

CONCLUSIONS

This study shows that field match regions can be detected and quantified (mm) by taking deconvolved Cherenkov images and using their square root/product image to create steep intensity gradients, causing match lines to stand out. This approach offers a high sensitivity detection method which could quantify match line variability and errors *in vivo*.

Future work includes correcting blurring introduced by breathing motion, as this also blurs the edges of the field and influences the integrity and signal gradients around the match line.

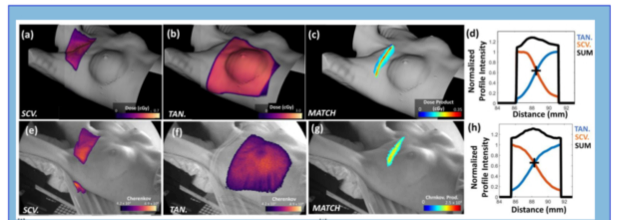

FIGURE 8: The techniques applied for Patient 1 in Figure 7 are also applied here for a patient treated using wet-towel bolus. It was determined that the bolus did not substantially compromise the applicability of the techniques proposed in this study, and the range of gaps and overlaps spanned 2.5 mm surrounding the expectation from the treatment plan.

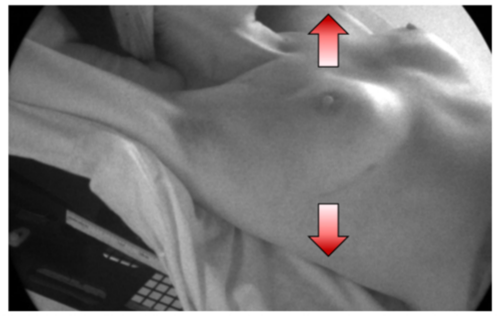

FIGURE 9: In free-breathing treatments, the field edge in the Cherenkov image is blurred from patient chest movement. Future work focuses on summing frames temporally centered around in vivo fiducials, to correct blurring.

REFERENCES

[1] Hachadorian, R., Borza, V., Jermyn, M., Jarvis, L., Bruza, P., Gladstone, D., & Pogue, B. (2019, June). Macroscopic Tissue Attenuation Corrections to Quantify Cherenkov Intensity Remission in Radiotherapy Using Measures of Reflectance and X-Ray CT Number. In MEDICAL PHYSICS (Vol. 46, No. 6, pp. E365-E366). 111 RIVER ST, HOBOKEN 07030-5774, NJ USA: WILEY.
[2] Zhang, R., J.M. Andreozzi, D.J. Gladstone, W.L. Hitchcock, A.K. Glaser, S. Jiang, B.W. Pogue, and L.A. Jarvis, Cherenkoscopy based patient positioning validation and movement tracking during post-lumpectomy whole breast radiation therapy. Phys Med Biol, 60(1): p. L1-14 (2015).
[3] Banaei, A., Hashemi, B., & Bakhshandeh, M. (2015). Comparing the monoisocentric and dual isocentric techniques in chest wall radiotherapy of mastectomy patients. Journal of applied clinical medical physics, 16(1), 130-138.
[4] Singh A, Arora D (2015) A Case of Breast Cancer Recurrence at the "Match Line". J Blood Lymph 1: 101.
[5] Niroomand-Rad, A., Blackwell, C. R., Coursey, B. M., Gall, K. P., Galvin, J. M., McLaughlin, W. L., ... & Soares, C. G. (1998). Radiochromic film dosimetry: recommendations of AAPM radiation therapy committee task group 55. Medical physics, 25(11), 2093-2115.
[6] Jursinic, P. A. (2007). Characterization of optically stimulated luminescent dosimeters, OSLDs, for clinical dosimetric measurements. Medical physics, 34(12), 4594-4604.
[7] Black, P. J., Velten, C., Wang, Y. F., Na, Y. H., & Wuu, C. S. (2019). An investigation of clinical treatment field delivery verification using cherenkov imaging: IMRT positioning shifts and field matching. Medical physics, 46(1), 302-317.
[8] Miao, T., Bruza, P., Pogue, B. W., Jermyn, M., Krishnaswamy, V., Ware, W., ... & Williams, B. B. (2019). Cherenkov imaging for linac beam shape analysis as a remote electronic quality assessment verification tool. Medical physics, 46(2), 811-821.
[9] Hachadorian, R.L., Bruza, P., Jermyn, M. et al. Imaging radiation dose in breast radiotherapy by X-ray CT calibration of Cherenkov light. Nat Commun 11, 2298 (2020). https://doi.org/10.1038/s41467-020-16031-z
[10] Ashraf, M. R., Bruza, P., Krishnaswamy, V., Gladstone, D. J., & Pogue, B. W. (2019). Time-gating to medical linear accelerator pulses: Stray radiation detector. Medical physics, 46(2), 1044-1048.
[11] Hojjatoleslami, S. A., Avanaki, M. R. N., & Podoleanu, A. G. (2013). Image quality improvement in optical coherence tomography using Lucy–Richardson deconvolution algorithm. Applied optics, 52(23), 5663-5670.
[12] Michalski, J.M., E.E. Klein, and R. Gerber, Method to plan, administer, and verify supine craniospinal irradiation. J Appl Clin Med Phys, 3(4): p. 310-6 (2002).
[13] McMahon, R.L., N.A. Larrier, and Q.J. Wu, An image-guided technique for planning and verification of supine craniospinal irradiation. J Appl Clin Med Phys, 12(2): p. 3310 (2011).

ACKNOWLEDGEMENTS

This work has been predominantly funded by NIH grant R01 EB023909 and supported by camera use and installation through R44 CA232879 and through the support of the Norris Cotton Cancer Center shared resources in P01 CA023108. We also acknowledge the hard work, dedication, and patience of the radiation therapists and patient care team in Dartmouth-Hitchcock Medical Center Radiation Oncology.

CONTACT INFORMATION

Rachael Hachadorian, MSc
PhD Candidate – Pogue Lab
Thayer School of Engineering
Dartmouth College
Rachael.L.Hachadorian.TH@dartmouth.edu
Lab: 603-650-1925
Cell: 858-243-8133

Prof. Brian Pogue, PhD
MacLean Professor of Engineering
Professor of Surgery, Geisel School of Medicine
Co-Director, Translational Engineering in Cancer Research Program, Norris Cotton Cancer Center
Brian.W.Pogue@dartmouth.edu
Lab: (603) 646-3861